A Study of Quantum Confinement Properties of Photogenerated Charges in ZnO Nanoparticles by Surface Photovoltage Spectroscopy

Lin Yanhong, Wang Dejun,* Zhao Qidong, Yang Min, and Zhang Qinglin

College of Chemistry, Jilin University, Changchun 130023, P.R. China

Received: October 23, 2003; In Final Form: December 29, 2003

The ZnO quantum dots (about 3 nm in average size) and the ZnO nanorods (about 80 nm in length and 14 nm in width) were synthesized by the sol−gel method. They were characterized by X-ray powder diffraction (XRD), transmission electron microscopy (TEM), UV−vis spectroscopy, and photoluminescence (PL) spectroscopy. The surface photovoltage (SPV) of ZnO nanoparticles was investigated by means of surface photovoltage spectroscopy (SPS) and field-induced surface photovoltage spectroscopy (FISPS), and the bands were identified. The results show that the SPV of ZnO nanoparticles are greatly different for their different sizes as a result of the quantum confinement effect. The ZnO quantum dots exhibit marked quantum confinement properties; that is, FISPS takes a high symmetry in the changes of the response intensity with the strengthening of the two opposed electric fields, and the FISPS response band always appears at about 369 nm, no matter what external electric field is applied. Whereas for the ZnO nanorods an asymmetry in its SPV response under the positive and negative electric field is observed, suggesting the existence of the bound excitons, which appears near the edge of the SPV response band.

Introduction

Functional materials are playing a more and more important role in science and technology for their unique optical, electrical, magnetic, and chemical properties. They are widely used in the area of solar energy conversion, surface sensitization and modification of semiconductors, nanoelectronics, etc.[1,2] Recently, much attention has been paid to ZnO owing to its wide band gap energy of 3.36 eV and a large exciton binding energy of 60 meV. ZnO nanoparticles, because of their larger specific surface, higher surface activity, and sensitivity to the surrounding environment, have become a most promising material in the manufacture of sensor devices.[3] Furthermore, depending on the superior luminescence and photoelectric properties, ZnO nanoparticles have been applied in making of transparent electrode in display dye-sensitized solar cell and the photoelectric devices of heterojunction structure, etc.[4−6] A lot of papers have appeared that explore the photoelectric properties and energy band structure of ZnO nanoparticles in relation to biologic oxygen sensors and lasers.[7,8] The application of ZnO nanoparticles is largely based on how much we know about the electronic structure and charge-transfer behavior at the surface or interface. However, to the best of our knowledge, few reports have been found.[9,10]

The SPV method is a well-established contactless and nondestructive technique for semiconductor characterization that relies on analyzing illumination-induced changes in the surface voltage. SPS is a effective tool to investigate the photophysics of excited states generated by absorption in the aggregate state.[11] SPV measurement features many advantages. For example, it has a very high sensitivity. The sensitivity of this method is about 10^8 q/cm^2, or about one elementary charge per 10^7 surface atoms, which exceeds that of conventional spectroscopies such as XPS and Auger spectroscopy by many orders of magnitude.[12] In addition, SPS is a kind of action spectrum. The information provided by SPS is about the properties of the sample surface layer (several atomic layers). This technique has been successfully employed for the study of the charge transfer in photostimulated surface interaction, dye sensitization processes, and photocatalysis.[12−14] On the basis of the principle of SPS, Dr. Wang's group developed a field-induced surface photovoltage technique, which can demonstrate the optoelectric properties of semiconductors under the effect of an external electric field.[15]

In this work, nanoparticles of ZnO with different sizes were prepared by the sol−gel method. Influence of size and excitation wavelength on the separation of photogenerated electron−hole pairs was investigated by means of SPS and FISPS. The relationship between size and photogenerated charge quantum confinement properties was also studied. This should be valuable for the practical application of ZnO nanoparticles in the field of chemical sensor in gas detecting system, photoluminescence, photocatalysis, etc.[13,16,17]

Experimental Section

Sample Preparation. The synthesis of ZnO quantum dots in this work is similar to that described in ref 18. Zinc acetate ($C_4H_6O_4Zn\cdot 2H_2O$ from Aldrich), absolute ethanol, and lithium hydroxide ($LiOH\cdot H_2O$ from Aldrich) were used as received without further purification. The procedure consists of two major steps. (1) Preparation of precursor: A 0.1 L ethanolic zinc acetate solution (0.1 M) was placed into a distillation flask fitted with a condenser and refluxed for 3 h at 80 °C under magnetic stirring. The condensate was collected continuously. At the end of this procedure, 0.04 L of precursor and 0.06 L of condensate were obtained. The precursor was immediately diluted to the original volume of 0.1 L with absolute ethanol and then cooled rapidly to room temperature. (2) Hydrolysis of precursor: A desired amount of lithium hydroxide powder was added to the diluted, cooled precursor solution (the concentration of LiOH

* Corresponding author: Tel +86-431-8499172; Fax +86-431-8499087; e-mail wangdj@mail.jlu.edu.cn.

10.1021/jp037201k CCC: $27.50
Published on Web 02/11/2004

is 0.14 M). The mixture was then hydrolyzed in an ultrasonic bath at about 0 °C for 20 min. Finally, the ZnO solution was filtered to remove dust and any undissolved lithium hydroxide. Thus, a transparent and stable colloidal solution 0.1 M was yielded. By adding a certain amount of hexane into the colloidal solution, a white precipitate was obtained and then was centrifuged, washed, and dried in a vacuum condition. The ZnO quantum dots powder was obtained. The preparation of ZnO nanorods was carried out as follows. The colloidal solution containing ZnO quantum dots prepared by the above method was first concentrated to 0.6 M and refluxed for 13 h. A certain amount of hexane was added. Finally, the precipitate thus obtained was centrifuged and dried under vacuum at 60−70 °C, yielding ZnO nanorods.

XRD, TEM, UV−vis, and PL Measurements. The as-prepared ZnO nanparticles were characterized by a XRD (XRD-6000, Shimadzu) employing graphite monochromatized Cu Kα radiation, a scanning rate of 4°/min and ranging from 20° to 70°. For XRD measurements, nanocrystal powder was placed on a glass sample holder. The morphologies and dimensions of the products were observed by TEM (Hitachi H-8100 IV). Dispersion of the as-prepared product in ethanol was conducted in an ultrasonic bath for half an hour. A drop was taken out and put on a copper mesh coated with a carbon film for a moment. Then the TEM measurement was performed. UV−vis spectra of colloidal suspensions were obtained on a CARY 100 spectrophotometer. PL spectroscopy of ZnO powders was obtained using an Edinburgh Analytical Instruments FS920 type visible−ultraviolet spectrophotometer with a 450 W xenon lamp at room temperature.

SPS and FISPS Measurements. The SPS instrument was made by ourselves. Monochromatic light was obtained by passing light from a 500 W xenon lamp (CHF XQ500W, Global xenon lamp power made in China) through a double-prism monochromator (Hilger and Watts, D 300 made in England). The slit width of entrance and exit is 1 mm. A lock-in amplifier (SR830-DSP, made in U.S.A), synchronized with a light chopper (SR540, made in U.S.A), was employed to amplify the photovoltage signal. The range of modulating frequency is from 20 to 70 Hz. The spectral resolution is 1 nm. The raw SPS data were normalized using the illuminometer (Zolix UOM-1S, made in China). The samples were studied without further treatment during the SPS and FISPS measurements, and the contact between samples and indium tin oxide (ITO) electrode is not ohmic contact since we carried out the measurement of surface photovoltage. The construct of the photovoltaic cell is a sandwich structure (see Figure 4, inset). It was ensured that the light penetrating depth was much less than the powder layer thickness. The obvious absorption of the ITO electrode was observed at 300−330 nm (see inset in Figure 3). The potential of the irradiated electrode with respect to the back electrode denotes the signs of the applied electrical field (see Figure 8).

Results and Discussion

A. Characterizations of the Samples. X-ray powder diffraction patterns of the samples A (ZnO quantum dots) and B (ZnO nanorods) are illustrated in Figure 1. Broadened diffraction peaks can be seen for sample A, indicating its very small grain size (about 14.6% of crystallinity obtained from the XRD system). Reflux of the concentrated solution, however, leads to the production of rodlike nanoparticles of sample B. It can be observed that the diffraction peaks of sample B are more intense and narrow than the ones of sample A. The diffraction peak 002 is sharpened, which is consistent with the implication of

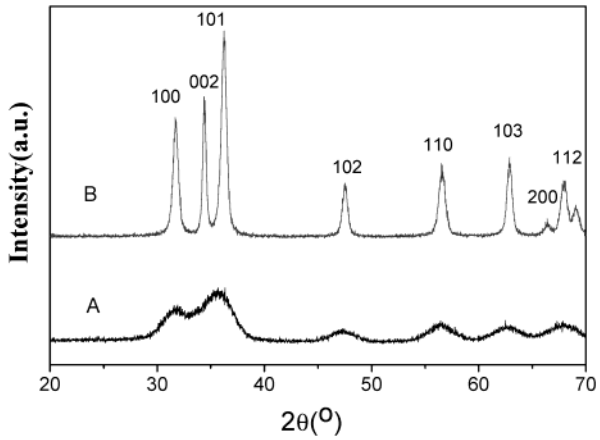

Figure 1. X-ray diffractogram of the ZnO quantum dots (A) and nanorods (B) prepared by the sol−gel approach. For the sake of clarity, the XRD curve for B was shifted upward.

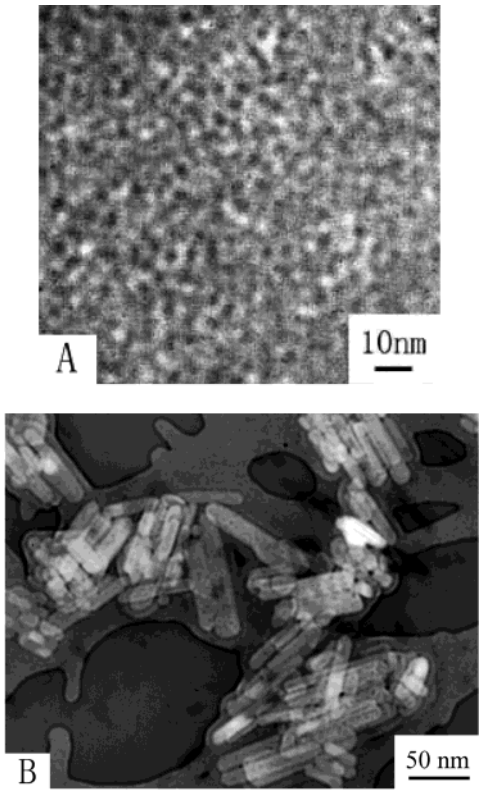

Figure 2. TEM images of the ZnO quantum dots (A) and nanorods (B).

the formation of the nanorods along the *c* axis. This means that the crystallinity of sample B improves greatly, reaching about 46.1%. The diffraction pattern and interplane spacings can be well matched to the standard diffraction pattern of wurtzite ZnO, demonstrating the formation of wurtzite ZnO nanocrystals. Scherrer line width analysis of shown peaks of sample A yields particle diameters around 3 nm, which is consistent with the TEM images. TEM images of samples A and B are shown in Figure 2. It is observed that the particles of sample A have a similar size and spherical shape. From Figure 2a the average size is estimated at 3 nm. For sample B, uniform rodlike single crystals can be seen and estimated approximately at 80 nm and 14 nm in average length and width, respectively (Figure 2b).

B. Analysis of SPS and FISPS. UV−vis absorption spectra of samples A (curve a) and B (curve b) are illustrated in Figure 3. It is seen that the absorption thresholds of the samples are

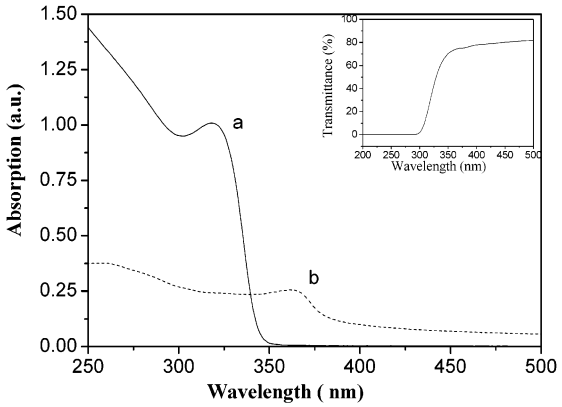

Figure 3. UV−vis absorption spectra of ZnO quantum dots (curve a) and nanorods (curve b). Inset: transmission spectrum of ITO.

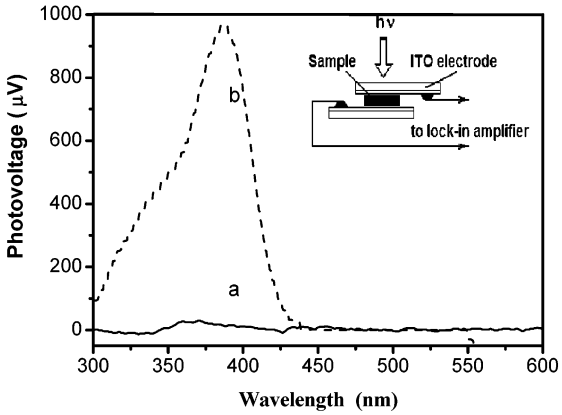

Figure 4. SPS of ZnO quantum dots (curve a) and nanorods (curve b). Inset: scheme of the structure of the photovoltaic cell.

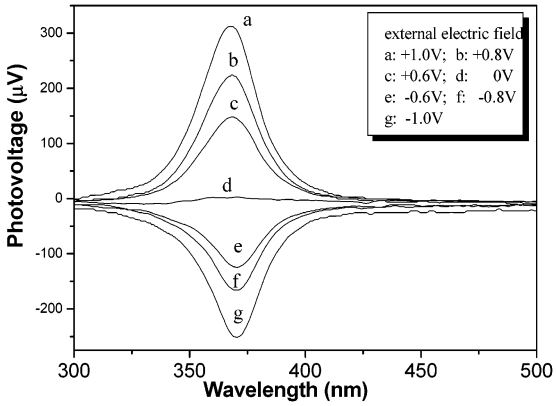

Figure 5. FISPS of ZnO quantum dots under different external electric fields.

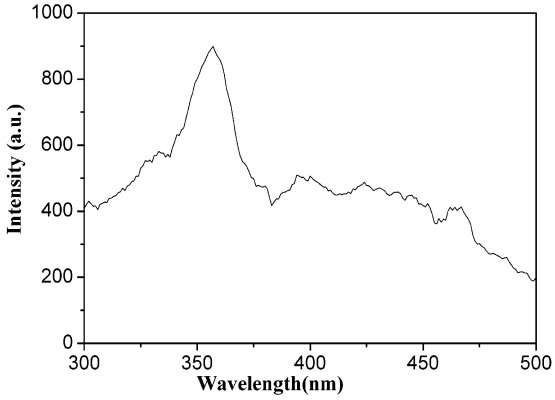

Figure 6. Excitation spectrum of 550 nm emission of ZnO quantum dots. The strongest green PL emission was observed when sample A was excited around 350 nm.

3.6 and 3.2 eV, respectively. The absorption spectra band blue shift is observed with the particles size decrease. At the same time the exciton absorption peak becomes more significant and blue shifts when the size decreases. A clear quantum confinement effect is exhibited.

SPS of samples A and B are shown in Figure 4. The SPV response of sample A is much weaker than that of sample B. The reason for this is mainly the difference in particles sizes. The particle sizes of sample A are so small that the energy band cannot be formed, and the electrons and holes move only in a potential well. It is reasonable to deduce that in an extremely small spherical particle (∼3 nm) the photogenerated electrons and holes cannot be effectively separated. As a result, sample A is unable to make a distinct SPV response. On the contrary, sample B has a higher crystallinity and larger average particle size (∼100 nm of long axis). Therefore, a perfect energy band can be formed, and the photogenerated charges can be distinctly separated by the built-in field (curve b). Two photovoltaic response bands in the range 300−410 nm were observed. Referring to the UV−vis absorption spectra, the bands P_{A1} at 300−350 nm and P_{A2} at 360−410 nm also show the band−band transition and exciton transition, respectively.

FISPS of sample A is shown in Figure 5. In Figure 5 there are three interesting points worthy of discussion. First, the SPV response intensity of A is very weak in the absence of external electric field. However, the SPV response intensity increases linearly with increasing electric field intensity as a positive field is applied. Besides, the SPV response intensity also increases when a negative field is applied but takes a reversal. Second, there is a high symmetry in the changes of the response intensity with the strengthening of the two opposed electric fields, and the FISPS response band always appears at about 369 nm, no matter what external electric field is applied. In general, this SPV response exhibits a character of quantum confinement of photogenerated charges in ZnO. Finally, from a comparison between Figure 3 and Figure 5 it is known that there is a pronounced absorption band in the range of 300−350 nm in UV−vis absorption spectrum for sample A but no corresponding SPV responses. In addition, the absorption in UV−vis corresponding to the SPV response peak (at 369 nm) is rather weak. Apparently these two results are contradictory to each other. Actually this is not the case. This seeming contradiction can be explained as follows. This phenomenon is related to the nature of luminescence, sensitivity of SPS technique, and the character of ZnO exciton absorption. The investigation on the luminescent nature of sample A reveals that sample A has the strongest green emission of 550 nm when excited around 350 nm (see Figure 6), which is consistent with the results of other groups.[18,19] This suggests that this absorption band makes little contribution to the SPV owing to its radiative transition from excited to ground states. That sample A exhibits strong SPV but weak absorption at 369 nm may be attributed to the sensitivity of SPS technique and the character of the exciton of ZnO. As a rule, the sensitivity of the SPV measurement is very high. So the SPV response can still be detected as long as the photogenerated charges can be effectively separated despite weaker absorption of the samples. In some papers, the band at 369 nm of sample A is attributed to the exciton absorption.[20−22] We know that the exciton binding energy of ZnO is about 60 meV. Guo et al. have observed the existence of excitons at room temperature.[22] The excitons are neutral since the photogenerated electrons and holes were limited in ZnO quantum dots. Hence, the SPV

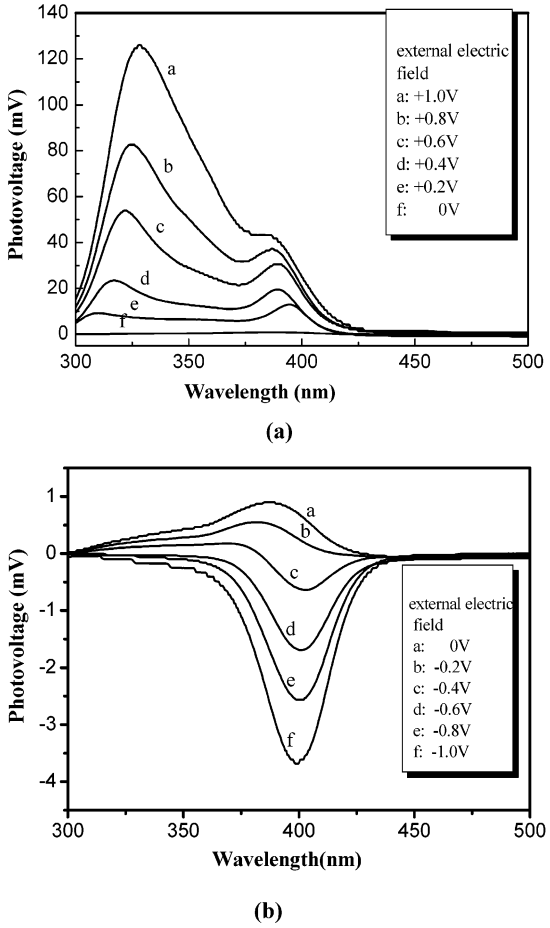

Figure 7. FISPS of ZnO nanorods under positive field (a) and negative field (b).

response in the absence of the electric field is weak. Under the action of external electric field the photogenerated electron−hole pairs were separated more effectively, and the charges cross the boundaries between nanoparticles. So the SPV response intensity increases greatly. From the above discussion we suggest that the absorption of sample A at 300−350 nm makes a contribution to the luminescence process. The SPV response at 369 nm should be attributed to the exciton transition and shows significant quantum confinement effects.

The FISPS of sample B is shown in Figure 7. To investigate the influence of built-in field on the SPV response, we have carried out the experiment of SPV technique with gas probe. We found that the change of SPV response took place under different ambients (be it air, other gases, or vacuum). In particular, we observed that the SPV response disappeared entirely when the samples were measured in a vacuum at 2×10^{-6} Torr (more details will be published elsewhere). So we suggest that the main driving force of the separation of the photogenerated electron−hole pairs comes from the built-in field produced by active particles. As is mentioned above, because of larger size of ZnO nanorods, perfect energy band structure has developed. Therefore, the photogenerated charges can be separated and diffuse to some extent and the SPV response can take place for sample B without an external electric field. FISPS of sample B under the positive electric field is shown in Figure 7a. It is obvious, on one hand, that the SPV response intensity increases with increasing positive electric field strength, indicating its n-type conduction character (see Figure 8 for an explanation). On the other hand, the SPS of sample B gives two pronounced SPV response bands in the range 300−410 nm.

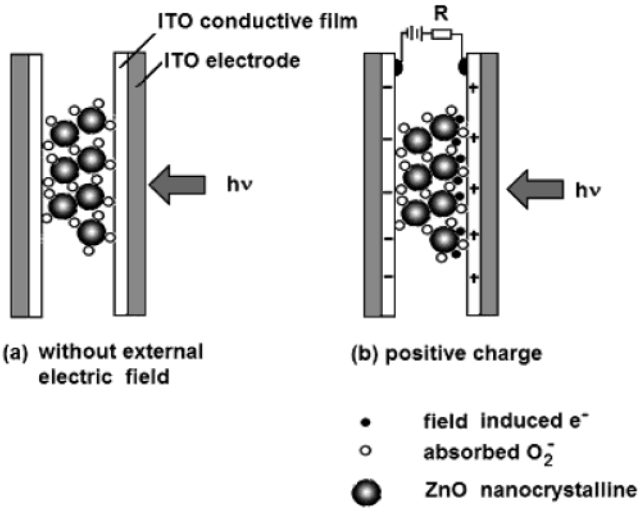

Figure 8. Scheme of the formation of built-in field after absorption of O_2 (a) and change in built-in field under external electric field (b).

The bands P_{B1} at 300−350 nm and P_{B2} at 360−410 nm are assigned to band-to-band transition and exciton transition, respectively. Furthermore, from this figure, it is found that the positions of the two bands shift with increasing positive electric field strength, and the shift directions of the peaks are different: red shift for P_{B1} and blue shift for P_{B2}. A model based on the Stark effect[23] can explain the red shift. The electrons in bulk on the irradiated side of the electrode move to the surface on the same side of the sample under the inducement of positive electric field (as is depicted in Figure 8b). The electron density at the top of valence band is enhanced with increasing electric field strength. The increment of state density will increase the probability of excited transition. Hence, two effects will be brought about with increasing electric field strength: the red shift of P_{B1} and the increasing SPV response intensity. As for the blue shift of P_{B2}, we analyze it on the basis of the FISPS principle. In general, bound exciton states can be formed in several modes,[24,25] such as interaction between exciton pairs and acceptor states (type A), interaction between exciton pairs and donor states (type B), exciton pairs generated by excited donor surface states (type C), exciton pairs produced when electrons are excited into acceptor surface states from valence band (type D), and so on. According to Figure 7, we suggest that P_{B2} should be attributed to bound excitons of type C. That is, the exciton pairs are generated when the donor surface states nearby the valence band of sample B are excited, and photogenerated electrons are injected into conduction band, leaving holes in the donor surface states. Compared to photogenerated electrons, holes in the surface states are significantly localized. And because surface states have an energy distribution, the localized holes have different levels of binding energy correspondingly. When the negative electric field is applied (Figure 7b), electrons of exciton pairs are pushed toward the bulk, leaving excess holes in the surface states. The exciton pairs are separated. Thus, SPV is produced, the intensity of which is proportional to the electric field intensity, and the position of the peak has no change with the negative electric field. When positive electric field is applied (Figure 7a), holes in the surface states are pushed toward the bulk, leaving excess negative charge at the surface. However, as the binding energy levels of the localized holes in surface states are different, more holes of higher binding energy levels transfer toward the bulk, and P_{B2} takes a seemingly blue shift with the increasing of the positive electric field intensity.

In a comparison between parts a and b of Figure 7, it is clearly seen that there is an asymmetry in the SPV response to positive and negative electric fields for P_{B2}. Both the changes of the intensity of SPV response and the shift of the peak position have asymmetry. The SPV response to the positive field is about an order of magnitude higher than that to the negative field. It follows that the SPV response for bound exciton under external electric field has an important character: SPV response changes asymmetrically with intensity and polarity of external electric field. It is also found that the intensity of the SPV response from the band-to-band transition under negative field is much weaker than that from the positive field. The factor affecting the SPV response is thought to be the built-in field. According to a model depicted in Figure 8, the strength of the built-in field will be weakened and even disappear and take a reverse in some cases, if a negative electric field is applied. Thereby, the intensity of SPV response is weakened first, and then it can take a reverse.

To elucidate the influence of external electric field on the SPV response intensity during the FISPS measurement, a model was suggested (see Figure 8). In preparation of oxide semiconductors, stoichiometric deviation often happens as a result of the escape of lattice oxygen, causing the increase of free electrons in the system.[26] Therefore, nanocrystals prepared such as ZnO are often n-type.[27] In the air, ZnO of n-type conduction can make part of the absorbed O_2 negatively charged, producing a built-in field at the surface of the particles. The built-in field is so oriented that the outer surface is negative and the space charge region (SCR) is positive. Under the built-in field, the photogenerated electron−hole pairs are separated. Naturally, the SPV response intensity should be proportional to the strength of the built-in field. Besides the absorbed O_2^- ion, the ZnO semiconductor of n-type can induce a large quantity of negative charges on the irritated side of the electrode. This process will strengthen the intensity of build-in field. Therefore, the SPV response intensity increases with increasing positive electric field. When a negative electric field is applied, the quantity of negative charge at the surface will be reduced, and the strength of the built-in field is weakened and even increases in opposite direction when the strength of the negative field is strong enough.

Conclusion

On the basis of our research the following conclusion can be drawn. The SPV of ZnO nanoparticles are quite different for their different sizes. For ZnO quantum dots the photogenerated charges exhibit marked quantum confinement properties. The SPV response band at 369 nm is assigned to the exiton transition, while the FISPS takes a symmetrical reversal as the external electric field is applied. The photovoltaic response intensity of ZnO nanorods is 2 orders of magnitude higher than that of quantum dots, and there exist two bands at 300−410 nm in SPV spectra of ZnO nanorods, caused respectively by the band-to-band transition and exciton transition. For the band-to-band transition, a red shift will take place if an external electric field is applied. This is explained to be a result of the Stark effect. The blue shift corresponding to the exciton transition occurs in the presence of an electric field. An asymmetry in its SPV response under the positive and negative electric field is observed, suggesting the existence of the bound excitons, which appears near the edge of the SPV response band. It is shown that the SPS and FISPS techniques are of great significance to the research on the charge-transfer behavior at the surface or interface in semiconductors.

Acknowledgment. We gratefully acknowledge financial support from the National Natural Science Foundation of China (Grant 20273027), the Research Fund for the Doctoral Program of Higher Education (RFDP) of China (Grant 20020183008), and the Nano-technique Fund of Jilin University, China.

References and Notes

(1) Robert, P.; Serge, P.; Jessica, K.; Michael, G. *J. Phys. Chem. B* **2002**, *106*, 7578.
(2) Park, N. G.; Schlichthörl, G.; Lagemaat, J.; Cheong, H. M.; Mascarenhas, A.; Frank, A. *J. Phys. Chem. B* **1999**, *103*, 3308.
(3) Liang, S.; Sheng, H.; Liu, Y.; Huo, Z.; Lu, Y.; Shen, H. *J. Cryst. Growth* **2001**, *225*, 110.
(4) Rensmo, H.; Keis, K.; Lindström, H.; Södergren, S.;Solbrand, A.; Hagfeldt, A.; Lindquist, S. E.; Wang, L. N.; Muhammed, M. *J. Phys. Chem. B* **1997**, *101*, 2598.
(5) Saito, N.; Haneda, H.; Sekiguchi, T.; Ohashi, N.; Sakaguchi, I.; Koumoto, K. *Adv. Mater.* **2002**, *14*, 418.
(6) Keis, K.; Bauer, C.; Boschloo, G.; Hagfeldt, A.; Westermark, K.; Rensmob, H.; Siegbahn, H. *J. Photochem. Photobiol. A: Chem.* **2002**, *148*, 57.
(7) Marian, Z.; Alexey, K.; Bernard, G.; Guillaume, M. *Phys. Status Solidi A* **2003**, *195*, 563.
(8) Kuveshni, G.; David, S. B.; Paul, O. B.; David, B.; Dave, W.; Dan, C. *Adv. Mater.* **2002**, *14*, 1221.
(9) Kronik, L.; Shapira, Y. *Surf. Interface Anal.* **2001**, *31*, 954.
(10) Du, H.; Cao, Y. A.; Bai, Y. B.; Zhang, P.; Qian, X. M.; Wang, D. J.; Li, T. J.; Tang, X. Y. *J. Phys. Chem. B* **1998**, *102*, 2329.
(11) Kronik, L.; Shapira, Y. *Surf. Sci. Rep.***1999**, *37*, 1.
(12) Gatos, H. C.; Lagowski, J.; Banisch, R. *Photogr. Sci. Eng.* **1982**, *26*, 24.
(13) Lenzmann, F.; Krueger, J.; Burnside, S.; Brooks, K.; Gratzel, M.; Gal, D.; Ruhle, S.; Cahen, D. *J. Phys. Chem. B* **2001**, *105*, 6347.
(14) Xie, T. F.; Wang, D. J.; Zhu, L. J.; Li, T. J.; Xu, Y. J. *Mater. Chem. Phys.* **2001**, *70*, 103.
(15) Wang, D. J.; Zhang, J.; Shi, T. S.; Wang, B. H.; Cao, X. Z.; Li, T. J. *J. Photochem. Photobiol. A: Chem.* **1996**, *93*, 21.
(16) Chatterjee, A. P.; Mitra, P.; Mukhopadhyay, A. K. *J. Mater. Sci.* **1999**, *34*, 4225.
(17) Chakrabarti, S.; Ganguli, D.; Chaudhuri, S. *J. Phys. D: Appl. Phys.* **2003**, *36*, 146.
(18) Spanhel, L.; Anderson, M. A. *J. Am. Chem. Soc.* **1991**, *113*, 2826.
(19) Sakohara, S.; Ishida, M.; Anderson, M. A. *J. Phys. Chem. B* **1998**, *102*, 10169.
(20) Chen, Y. F.; Bagnall, M. D.; Koh, H. J.; Park, K. T.; Hiraga, K.; Zhu, Z. Q.; Yao, T. *J. Appl. Phys.* **1998**, *84*, 3912.
(21) Cho, S.; Ma, J.; Kim, Y.; Sun, Y.; Wong, G. K. L.; Ketterson, J. B. *Appl. Phys. Lett.* **1999**, *75*, 2761.
(22) Guo, L.; Yang, S. H.; Yang, C. L.; Yu, P.; Wang, J. N.; Ge, W. K.; Wong, G. K. L. *Appl. Phys. Lett.* **2000**, *76*, 2901.
(23) Dijken, A. V.; Meulenkamp, E. A.; Vanmaekelbergh, D.; Meijerink, A. *J. Phys. Chem. B* **2000**, *104*, 4355.
(24) Alves, H.; Pfisterer, D.; Zeuner, A.; Riemann, T.; Christen, J.; Hofmann, D. M.; Meyer, B. K. *Opt. Mater.* **2003**, *23*, 33.
(25) Gutowski, J.; Presser, N.; Broser, I. *Phys. Rev. B* **1988**, *38*, 9748.
(26) Sukkar, M. H.; Tuller, H. L. *Adv. Ceram.* **1984**, *7*, 71.
(27) Lee, J. H.; Ko, K. H.; Park, B. O. *J. Cryst. Growth* **2003**, *247*, 119.